Title:
A Surface Unfolding Method for Bolus Shaping Using the Mass-spring Model

Authors:
Rui Li, lir34512@myumanitoba.ca, University of Manitoba
Qingjin Peng, Qingjin.Peng@umanitoba.ca, University of Manitoba
Harry Ingleby, hingleby@cancercare.mb.ca, CancerCare Manitoba
David Sasaki, dsasaki@cancercare.mb.ca, CancerCare Manitoba

Keywords:
Surface Unfolding, Bolus Shaping, Mass-spring Model

DOI: 10.14733/cadconfP.2019.263-267

Introduction:
Bolus is a sheet of material used in the high-energy radiotherapy to smooth patients' skin for a desired dose distribution [4]. The bolus should be close to the patient underlying tissue without air gaps to achieve a good therapeutic effect. A manual bolus shaping process is mainly used in clinic by cutting commercial material into two-dimensional (2D) shapes of the targeted body area and then wrapping into a three-dimensional (3D) shape to cover the patient surface. The bolus produced in this way is inaccurate and time-consuming. Digital technologies can improve product development such as applications in garment industry for efficient and accurate clothing making. 3D garments models are built based on human body data and then unfolded into 2D patches. Clothing materials are cut based on the 2D patches and then sewed into 3D garments [3]. The goal of unfolding a non-developable surface is to reduce errors from an original 3D surface to its unfolded 2D patches. Wang et al applied a mass-spring model in the unfolding process of mesh surfaces to optimize unfolded 2D patches [5]. Length and area errors were used as measures of unfolding accuracy. Li et al improved the mass-spring model by adding crossed springs for the speed optimization. Triangle strips were proposed to reduce the number of iterations in the process [1]. To reduce complexity of traditional mass-spring models, Liu et al simplified the mass-spring model using a hierarchy unfolding process to increase efficiency of the process [2].

Inspired the surface unfolding process in garment industries, a surface unfolding process is proposed based on the mass-spring model to unfold human surfaces for bolus shaping. To improve the unfolding efficiency from a 3D surface to 2D patches, triangle crossings are used to reduce the number of iterations. A mass-spring model with crossed springs is introduced for the optimization of 2D patches to reduce the deformation and distortion of unfolded surfaces. To improve efficiency in the contour optimization of 2D patches, a disturbing spring is added into the mass-spring model with crossed springs to change the shape of 2D patches. Using the proposed method, a bolus shaping process is developed for improving bolus shaping efficiency and accuracy.

Main Idea:
The proposed process of unfolding a 3D surface into 2D patches is first to fix a triangle of the 3D surface on a 2D flat datum and then transfer other nodes of the 3D surface onto the 2D datum with the less deformation. The transferring process starts at neighboring nodes of the fixed triangle working on a layer by layer process until all nodes are located in the 2D datum. To reduce deformation from the 3D surface to 2D patches, an energy model is applied to adjust the position of nodes in the 2D datum.

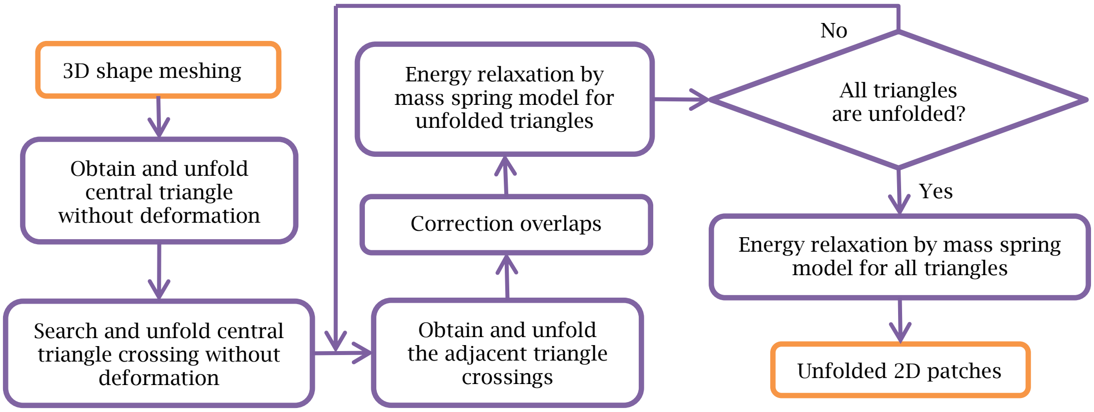

Fig. 1: Flowchart of the proposed method.

Triangle strips can improve efficiency of the surface unfolding process [1]. However, if the number of vertexes in a surface is large, its unfolding efficiency will be affected. To improve the unfolding efficiency, a triangle crossing is proposed to reduce the number of iterations in the coordinate transformation process. A crossed spring based mass-spring model is applied to optimize initial 2D patches to reduce deformation and distortion between the 3D surface and unfolded 2D patches. To increase efficiency of the optimal search, a disturbing spring is added in the mass-spring model to correct deformation in the shape and contour. The proposed process is illustrated in Fig. 1.

Implementation

The first step selects a central triangle to unfold it without deformation. Labels of boundary vertexes are defined as 0. Labels are then increased based on connections of nodes layer by layer. The triangle with the largest total label value is chosen as a central triangle.

A triangle crossing is proposed to increase the number of triangles unfolded in each unfolding step to reduce the number of iterations in the coordinate transformation process. Fig.2 shows the sequence of triangle crossings, where the pink crossing is the central triangle crossing and other triangles are adjacent triangle crossings. The weight center of the central triangle is calculated and several unfolding directions are defined through the weight center of the central triangle. After unfolding triangles pass through each unfolding direction, the total number of triangles in each unfolding direction is calculated. The unfolding direction with most triangles is chosen as main stripe. The main stripe and its vertical direction are composed as the central triangle crossing. The central triangle crossing is unfolded with no deformation. To unfold adjacent triangle crossings, targeted adjacent triangles are obtained firstly, which are 3D triangles having common vertexes with unfolded triangles. Inner angles of targeted triangles are calculated and used to find 2D positions of 3D vertexes in targeted adjacent triangles.

A mass-spring model with crossed springs as shown in Fig.3 is applied to control the shape of triangular meshes [1]. The crossed spring based mass-spring model has a high efficiency because a tension spring connects to two masses along with an edge, which can correct the length deformation of the edge. In addition, a crossed spring connects to two masses by crossing an edge where the two masses are on the edge's neighboring triangles.

The movement of node v_0 is restricted by spring force $f(Q_0, Q_i)$ from virtual springs. For each node v_i, the total spring force $\vec{f}(Q_i)$ is calculated as follows.

$$\vec{f}(Q_i) = \sum_{j=1}^{N} c(\left|Q_i Q_j\right| - D_{P_i P_j})\vec{n}_{Q_i Q_j} \tag{1}$$

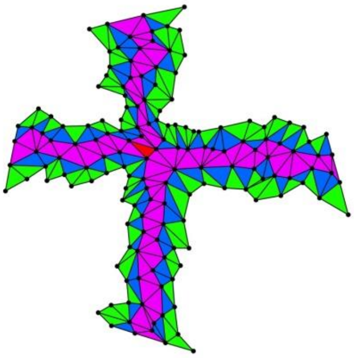

Fig. 2: Schematic diagram of triangle crossings.

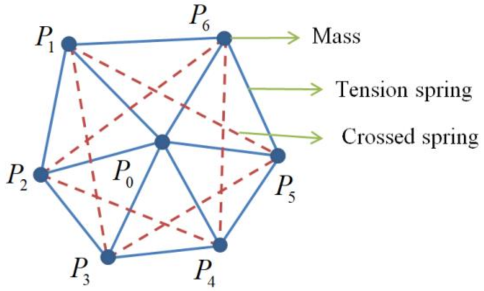

Fig. 3: Mass-spring model with crossed springs.

Where c is the stiffness coefficient; $|Q_iQ_j|$ is the length between unfolded nodes Q_i and Q_j in 2D patches; $D_{P_iP_j}$ is the distance between original nodes P_i and P_j in a 3D surface; $\vec{n}_{Q_iQ_j}$ is the force direction; N is the number of one-ring neighboring nodes for Q_i.

The Lagrange equation is used to release energy in the mass-spring model and solved by Euler's method. According to Newton's law, acceleration $\ddot{x}_i$ at node Q_i can be calculated as follows.

$$\ddot{x}_i(t) = \frac{f_i(t)}{m_i} \tag{2}$$

Position $x_i(t_{n+1})$ and velocity $\dot{x}_i(t_{n+1})$ at step n+1 can be calculated based on position $x_i(t_n)$, velocity $\dot{x}_i(t_n)$ and acceleration $\ddot{x}_i(t_n)$ at a time step n are calculated by Eqns. (3) and (4). The new spring force is updated using Eqn. (1) based on results in Eqn. (4). The objective of optimization is to minimize the total energy of the whole triangular surface.

$$\dot{x}_i(t_{n+1}) = \dot{x}_i(t_n) + \Delta t \cdot \ddot{x}_i(t_n) \tag{3}$$

$$x_i(t_{n+1}) = x_i(t_n) + \Delta t \cdot \dot{x}_i(t_n) + \frac{1}{2}\Delta t^2 \cdot \ddot{x}_i(t_n) \tag{4}$$

Shapes and contours of 2D patches have a significant impact on the accuracy of their folding back to the 3D shape. Thus, if the original unfolded patches have large deformation in shapes and contours, it is difficult to obtain an optimal result. A disturbing spring is then added in some important parts of 2D patches such as the length, width and contour to improve optimization results.

Two boundary vertexes v_{b1} and v_{b2} are linked by a disturbing spring. If v_{b1} is fixed, the movement of node v_{b2} is restricted by the spring force $f(v_{b1}, v_{b2})$ from springs and calculated by Eqn. (5).

$$\vec{f}(v_{b2}) = c\left(\sum|v_{bi}v_{bj}| - \sum D_{bibj}\right)\vec{n}_{v_{b1}v_{b2}} \tag{5}$$

Where c is the stiffness coefficient; $\sum|v_{bi}v_{bj}|$ is the sum length between unfolded nodes v_{b1} and v_{b2} in 2D patches; $\sum D_{bibj}$ is the sum distance between original nodes v_{b1} and v_{b2} in a 3D surface; $\vec{n}_{v_{b1}v_{b2}}$ is the force direction. Newton's law is used to calculate the new position of node v_{b2}. With the disturbing spring, the deformation in 2D patches can be reduced, and efficiency of the optimization process is improved.

To evaluate the accuracy of unfolded 2D patches, two types of errors are identified including the length error EL and area error EA as follows.

$$\mathrm{EL} = \frac{\sum|L - L_0|}{\sum L_0} \tag{6}$$

$$\mathrm{EA} = \frac{\sum |A - A_0|}{\sum A_0} \tag{7}$$

Where L_0 and A_0 are the edge length and triangle area on the triangular mesh 3D surface. L and A are the corresponding edge length and triangle area for unfolded 2D patches, respectively.

In the unfolding process, overlaps of 2D patches may be generated as the accumulation of deformations when more triangles are unfolded. Two methods are used to avoid overlapping. First one is a local algorithm for searching and optimizing overlaps. The other applies the energy release by the mass-spring model to reduce deformation of each triangle crossing in the unfolding process.

Case study

The surface unfolding process is coded in Matlab 2017. Two cases including a hemisphere model and a multi-patches nose model are unfolded using the proposed process. Results are shown in Tab. 1. Fallentability is applied to indicate the developable ability [6]. A smaller surface fallentability means the surface can be unfolded into 2D patches with less deformation and distortion.

Hemisphere is an undevelopable surface with the fallentability 5.9397. After the final energy release, the length error EL is decreased from 0.1231 to 0.0955 and the area error EA is decreased from 0.2213 to 0.1544. The energy release therefore improves the unfolding accuracy significantly.

As an irregular surface of the human body, a nose was scanned using a 3D scanner to obtain its 3D data. The data were then modeled to make a 3D printed model for evaluation of the bolus covering accuracy. The nose model is segmented into 4 parts to reduce the value of fallentability as shown in Fig. 4(a). The total fallentability of the nose model is 7.9636. The multi-patches include 4 parts with fallentability 1.6460, 2.7243, 1.7255 and 1.6917, respectively. 4 parts of the nose model are unfolded using the proposed method and shown in Fig. 4(b). The length errors EL for 4 parts are 0.0093, 0.0227, 0.0073 and 0.0075, respectively. The area errors EA are 0.0194, 0.0479, 0.0164 and 0.0186, respectively.

To further test and verify performance of the proposed unfolding process, a paper-made bolus is formed using the unfolded nose patches. The bolus is covered on the 3D printed nose model to find air gaps between the bolus and nose using a 3D laser scanner. Fig. 4(c) shows the paper bolus covering on the 3D printed nose model. The scanned surface of the 3D nose model is aligned with the scanned model surface. Differences are measured using the Control X tool. Fig. 5 shows air gaps between two models, where (a) is the 3D deviation; (b) shows the sectional view of symmetry plane of the model, and (c) is the sectional view of plane in the nose bridge. The maximum air gap calculated by summing the absolute value of the lower and upper deviations is 2.1501 mm.

Conclusions:

To obtain accuracy 2D patches for bolus shaping, a 3D surface unfolding method was proposed. Triangle crossings were proposed to improve the efficiency of iterations. A disturbing spring was added in the mass-spring model to correct the deformation in shapes and contours. Two case examples were tested to verify the proposed method. Results show that the solution meets requirements of bolus shaping.

Example	Fallentability	Node no.	Edge no.	Triangle no.	EL (%)	EA (%)
Hemisphere without final energy release	5.9397	444	1291	848	0.1231	0.2213
Hemisphere					0.0955	0.1544
Multi-patches nose model part 1	1.6460	886	2522	1637	0.0093	0.0194
Multi-patches nose model part 2	2.7243	1598	4578	2990	0.0227	0.0479
Multi-patches nose model part 3	1.7255	811	2344	1534	0.0073	0.0164
Multi-patches nose model part 4	1.6917	843	2431	1589	0.0075	0.0186

Tab. 1: Length errors and area errors of the unfolded models.

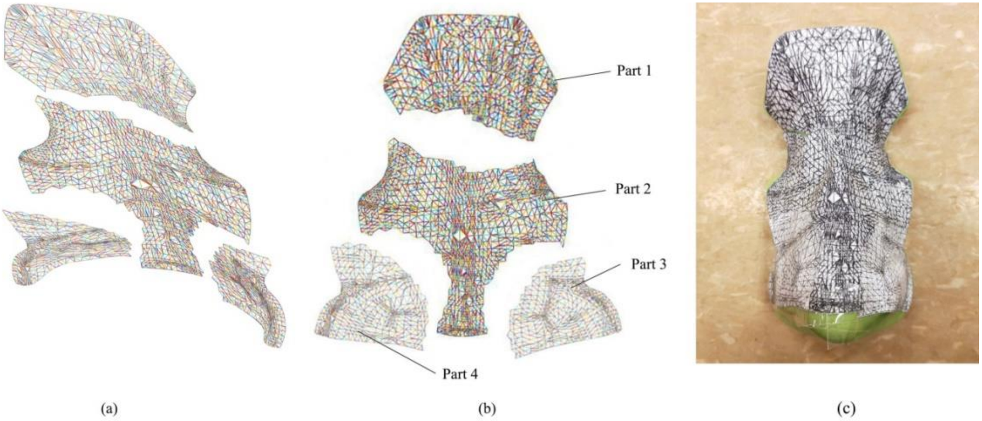

Fig. 4: A nose model and bolus. (a) 3D models, (b) 2D models, (c) Bolus covering on the 3D printed nose model.

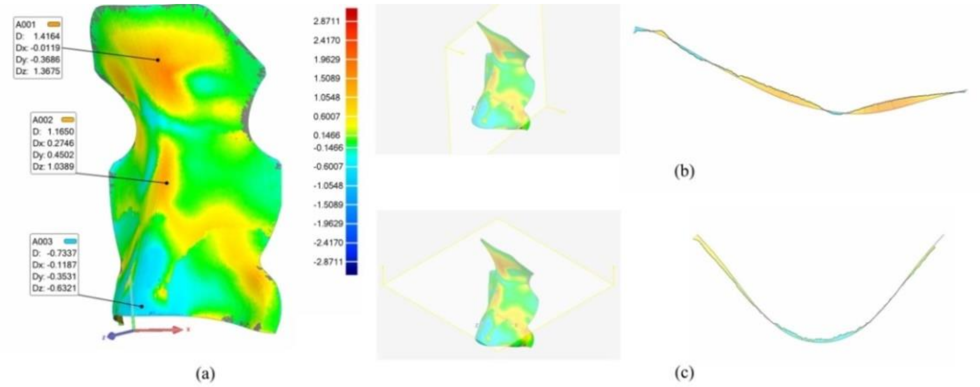

Fig. 5: Air gaps between the nose model and bolus. (a) 3D deviation, (b) Sectional view of symmetry plane of the nose model, (c) Sectional view of plane in the bridge of nose.

References:

[1] Li, J.; Lu, G.; Zhang, D.; Sakaguti, Y.: Searching a 3D region for surface trimming, International Journal of Advanced Manufacturing Technology, 30(11–12), 2006, 1093–1100. https://doi.org/10.1007/s00170-005-0158-y

[2] Liu, Q.; Xi, J.; Wu, Z.: An energy-based surface flattening method for flat pattern development of sheet metal components, International Journal of Advanced Manufacturing Technology, 68(5–8), 2013, 1155–1166. https://doi.org/10.1007/s00170-013-4908-y

[3] Thomassey, S.; Bruniaux, P.: A template of ease allowance for garments based on a 3D reverse methodology, International Journal of Industrial Ergonomics, 43(5), 2013, 406–416. https://doi.org/10.1016/j.ergon.2013.08.002

[4] Vyas, V.; Palmer, L.; Mudge, R.; Jiang, R.; Fleck, A.; Schaly, B.; Charland, P.: On bolus for megavoltage photon and electron radiation therapy, Medical Dosimetry, 38(3), 2013, 268-273. https://doi.org/10.1016/j.meddos.2013.02.007

[5] Wang, C. C. L.; Smith, S. S.-F.; M.F.Yuen, M.: Surface flatting based on energy model, Computer-Aided Design, 34, 2002, 823–833. https://doi.org/10.1016/S0010-4485(01)00150-6

[6] Wang, C. C. L.: Towards flattenable mesh surfaces, Computer-Aided Design, 40(1), 2008, 109–122. https://doi.org/10.1016/j.cad.2007.06.001